Laser Ablation Simulation Including Time Dependent Atomic Processes

Hiroyuki Furukawa

Institute for Laser Technology, 1-8-4 Utsubo-honmachi, Nishi-ku, Osaka, 550-0004, Japan;
E-mail: ran@ile.osaka-u.ac.jp, Telephone: +81 6 6879 8789

An integrated Laser Ablation Fluid RAdiation simulation Code (LAFRAC) has been developed to estimate behaviors of highly energetic ions and neutral particles from laser produced plasmas, and to estimate ionization and recombination processes. Neutral particles cannot be controlled by electric and/or magnetic forces. Therefore, estimation of the number of neutral particles and mitigation of them is very important.

LAFRAC includes effects of time dependent population kinetics, phase transition from liquid to neutral gas to partially ionized plasma, detail laser absorption processes, hydrodynamics, and radiation transport, to describe ablation phenomena with recombination and ionization processes, phase transition and properties of emission plasmas.

DOI: 10.2961/jlmn.2006.03.0011

Keywords: simulation, time dependent population kinetics, phase transition, neutral gas, detail laser absorption, radiation transport

1. INTRODUCTION

Laser ablation can be used for various applications, such as diagnostics of target composition, micro structure processing, removal of small space debris, radioactive surface cleaning, and laser-produced plasma (LPP) light sources. In LPP light sources, highly energetic particles are produced by laser ablations.

An integrated Laser Ablation Fluid RAdiation simulation Code (LAFRAC)[1] has been developed to estimate behaviors of highly energetic ions and neutral particles from laser produced plasmas, and to estimate ionization and recombination processes. Neutral particles cannot be controlled by electric and/or magnetic forces. Therefore, estimation of the number of neutral particles and mitigation of them is very important.

LAFRAC includes effects of time dependent population kinetics[2], phase transition[3] from liquid to neutral gas to partially ionized plasma, detail laser absorption processes[4], hydrodynamics, and radiation transport, to describe ablation phenomena with recombination and ionization processes, phase transition and properties of emission plasmas. Fig. 1 shows the schematic diagram of LAFRAC.

In section 2, basic equations of LAFRAC are described. In section 3, we summarize simulation results and discuss.

2. BASIC EQUATIONS OF LAFRAC[1]

2.1 Main Program of LAFRAC

Main program of LAFRAC consists of time dependent population kinetics, detail laser absorption and reflection, phase transitions from liquid to gas to plasma, ablation process, hydrodynamics, and radiation transport of X-ray. In this paper, this program is named 'LASP (Laser Ablation Simulation Program)'.

2.2 Population Kinetics[2]

In many hydrodynamics simulation code, ionization degree Z* is determined under the condition of ionization equilibrium, But in laser ablation produced corona plasmas, ionization equilibrium condition is not always formed. Fig. 1 shows 3-body and radiative recombination rates for the case (a) $n_i=10^{19}$ cm^{-3}, T_e=50 eV (b) $n_i=10^{17}$ cm^{-3}, T_e=50 eV using hydrogen like atom model[5].

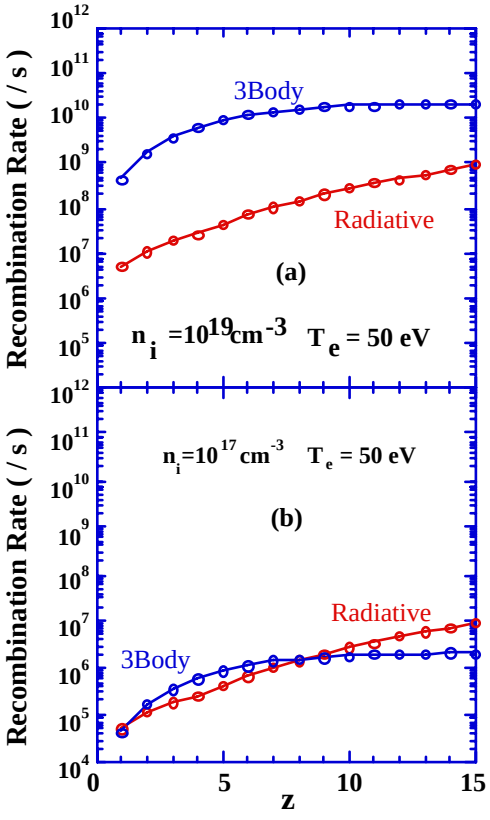

Fig. 1 3-body and radiative recombination rates for the case, (a) $n_i=10^{19}$ cm^{-3}, T_e=50 eV, (b) $n_i=10^{17}$ cm^{-3}, T_e=50 eV.

The horizontal axis stands the charge , and vertical axis stands recombination rates. As shown in Fig. 1, recombination time (defined as 1 / recombination rate) is not sufficiently shorter than laser pulse durations (for example 1

ns). Time dependent population kinetics equations have to be solved.

Populations of z charge ions N_z are calculated as follows[2].

$$\frac{dN(x,t,z)}{dt} = I(z-1\rightarrow z)N(x,t,z-1) + R(z+1\rightarrow z)N(x,t,z+1) - I(z\rightarrow z+1)N(x,t,z) - R(z\rightarrow z-1)N(x,t,z) \quad (1)$$

where I is ionization rate and R is recombination rate.

In LAFRAC, I relate populations between configuration i and j by Bolztmann equation.

$$N(x,t,z,j) = N(x,t,z,i)\frac{g(z,j)}{g(z,i)}\exp\left(-\frac{E_{ij}}{k_B T_e}\right) \quad (2)$$

$$\sum_j N(x,t,z,j) = N(x,t,z) \quad (3)$$

where g is statistical weight, k_B is Boltzmann constant, T_e is electron temperature, E_{ij} is energy gap between configuration i and j. In LAFRAC, energy levels are calculated by new screened hydrogen model with l-splitting developed by Dr. Nishikawa[6].

2.3 Energy Equations

2.3.1 In Liquid

Internal energy of liquid U_l is defined as follows.

$$U_l(x,t) \equiv \rho_l \left\{ \int_{T_0}^{T(t)} C_l\left(x, T(x,t)\right)dT + \Delta_l(x,t) \right\} \quad (4)$$

where ρ_l is mass density of liquid, C_l is specific heat of liquid, Δ_l is latent heat.

Time and spatial evolutions of U_l are obtained by following equation

$$\frac{\partial U_l(x,t)}{\partial t} = \nabla\cdot\left(\kappa_\ell \nabla T_l(x,t)\right) + Q_L(x,t) + Q_X(x,t) \qquad x_v < x < x_{\max} \quad (5)$$

where κ_l is thermal conductivity, Q_L is heat quantity due to absorption of laser, Q_x is heat quantity due to absorption of X-ray, and T_l is temperature of liquid.

Critical internal energy for peeling is given as follows

$$U_l^{crt} = \rho_l \left\{ \int_{T_0}^{T_{vap}} C_l(x,T)\,dT + L_v \right\} \quad (6)$$

If $U_l > U_l^{crt}$, peeling will occur. Here L_v is latent heat of vaporization, T_{vap} is vaporization temperature

2.3.2 In Ablated Materials

In many former radiation hydrodynamics simulation codes, one fluid and two temperature, total electrons (free electrons and bound electrons) and ions, approximations are adopted. But these approximations are not applied to high Z materials. Energy equations of free electrons and bound electrons should be separated.

Energy equation of free electrons is as follows.

$$\rho(x,t)c_v^{(fe)}\frac{\partial T_{fe}(x,t)}{\partial t} = -\nabla\cdot q_{fe}(x,t) - \gamma\left(T_{fe}-T_i\right) - P_{th}^{(fe)}(x,t)\nabla\cdot v(x,t) + Q_L^{fe}(x,t) + Q_{rad}^{fe}(x,t) + Q_{col}^{fe}(x,t) \quad (7)$$

$$P_{th}^{(fe)} = T_{fe}\left(\frac{\partial P^{(fe)}}{\partial T_{fe}}\right) \quad (8)$$

where v is velocity of fluid, fe stands free electron, i stands ion, T is temperature, P is pressure, q_{fe} is thermal flow due to free electrons, γ is relaxation constant of temperatures between free electrons and ions. Q^{fe}_L is heat quantity due to absorption of laser by free electrons, Q^{fe}_{rad} is heat quantity due to absorption of X-ray by free electrons, Q^{fe}_{col} is energy due to 3-body recombination and collisional ionization.

Energy equation of bound electrons is as follows,

$$\frac{\partial n_i \varepsilon_{be}(x,t)}{\partial t} = -P^{(be)}(x,t)\nabla\cdot v(x,t) - E_{be-i} + Q_L^{be}(x,t) + Q_{rad}^{be}(x,t) - Q_{col}^{fe}(x,t) \quad (9)$$

where n_i is number density of ions, ε_{be} is energy of bound electrons of an ion, $E_{be\text{-}i}$ is relaxation energy from bound electrons to ions.

Energy equation of ions is as follows

$$\rho(x,t)c_v^{(i)}\frac{\partial T_i(x,t)}{\partial t} = -\nabla\cdot q_i(x,t) + \gamma\left(T_{fe}-T_i\right) + E_{be-i} - P_{th}^{(i)}(x,t)\nabla\cdot v(x,t) \quad (10)$$

where q_i is thermal flow due to ions.

Heat quantities due to absorption of X-ray by free electrons and bound electrons are as follows.

$$Q_{rad}^{fe}(x,t) = -\int 4\pi\left[j_\nu^{ff}(x,t) + j_\nu^{fb}(x,t)\right] - \left[\kappa_\nu^{ff}(x,t) + \kappa_\nu^{bf}(x,t)\right]cE_\nu(x,t)\,d\nu - \sum_{z=0}^{Z-1} I_{z+1}\alpha_{ioniz}^{photo}N_z \quad (11)$$

$$Q_{rad}^{be}(x,t) = -\int 4\pi\, j_\nu^{bb}(x,t) - \kappa_\nu^{bb}(x,t)cE_\nu(x,t)\,d\nu + \sum_{z=0}^{Z-1} I_{z+1}\alpha_{ioniz}^{photo}N_z \quad (12)$$

where I_z is ionization energy, j is emissivity and κ is opacity, and α stands rate coefficient[2].

Energy due to 3-body recombination and collisional ionization is as follows.

$$Q_{col}^{fe}(x,t) = \sum_{z=1}^{Z} I_z\alpha_{rec}^{3body}N_z - \sum_{z=0}^{Z-1} I_{z+1}\alpha_{ioniz}^{col}N_z \quad (13)$$

2.4 Equation of Motion

Equation of motion of ablation surface (the boundary of liquid and neutral gas or plasma) is as follows[3].

$$\frac{\partial}{\partial t}x_v(t) = \sqrt{k_B T_v / m_i}\cdot\exp\left(-m_i L_v / k_B T_v\right) \quad (14)$$

$$\frac{\kappa_l}{\rho_l}\frac{\partial T_l(x,t)}{\partial x}\bigg|_{x=x_v} = L_v\frac{\partial}{\partial t}x_v(t) \quad (15)$$

$$T_v = T_l\left(x_v(t)\right) \quad (16)$$

where m_i is mass of an ion, x_v is ablation surface, T_v is temperature of ablation surface

Under the consideration of one fluid and three energy equations, equation of motion of ablated materials is written as follows.

$$\rho(x,t)\frac{dv(x,t)}{dt} = -\nabla\left[P_e^{(fe)}(x,t) + P_i(x,t) + P_{nv}(x,t)\right] \quad (17)$$

where ρ stands mass density of ablated materials, P_{nv} is numerical viscosity.

2.5 Radiation Transport

In LAFRAC, radiation flux is obtained using multi group diffusion approximation

$$\rho(x,t)\frac{d}{dt}\left(\frac{E_\nu(x,t)}{\rho(x,t)}\right) = -\nabla\cdot\left(F_\nu(x,t) - v\,E_\nu(x,t)\right) + 4\pi\ j_\nu(x,t) - c\,\kappa_\nu(x,t)E_\nu(x,t) \quad (18)$$

$$F_\nu(x,t) = -\frac{c}{\frac{\left|\nabla E_\nu(x,t)\right|}{E_\nu(x,t)} + 3\kappa_\nu(x,t)}\nabla E_\nu(x,t) \quad (19)$$

where E_v is radiation energy density, F_v is radiation flux.

3. RESULTS AND DISCUSSIONS

A laser ablation simulation using LAFRAC is performed. In this simulation, laser peak intensity is 10^{11} W/cm^2, pulse duration is 1.2 ns, and material is tin.

Fig. 2 shows total (includes neutral particles) ion number density profile, electron temperature profile and ionization degree profile at the time of laser peak**.** These profiles are different from those in the case of isothermal expansion (high laser intensity case) and adiabatic expansion (low laser intensity case). In the case of intermediate laser intensity (for example 10^{11} W/cm^2), simulation is very important and very difficult. Ion number density profile and electron temperature profile are in good agreements with calculating results and experimental results in ref. 6 and 7 qualitatively.

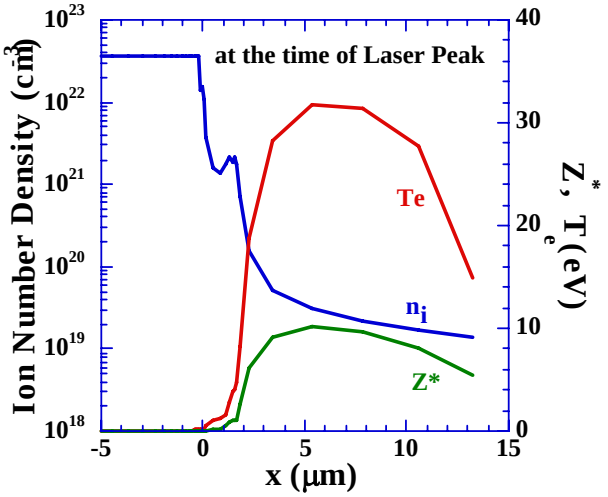

Fig. 2 Total (includes neutral particles) ion number density profile, electron temperature profile and ionization degree profile at the time of laser peak**.**

Fig. 3 shows time evolutions of number densities of each charges (includes neutral particles) of ablated materials. Fig. 3 (a) shows those of high energy (more than 500eV) particles, and (b) shows those of low energy (less than 500eV) particles. As shown in Fig. 3 (a), particles of which charges 8 to 11 are dominant for high energy part. As shown in Fig. 3 (b), particles of which charges 0 to 1 are dominant for low energy part. Note that number density of neutral particles of low energy part is almost100 times of that of particles of which charge 10 of high energy part. Almost of all ablated materials are neutral particles.

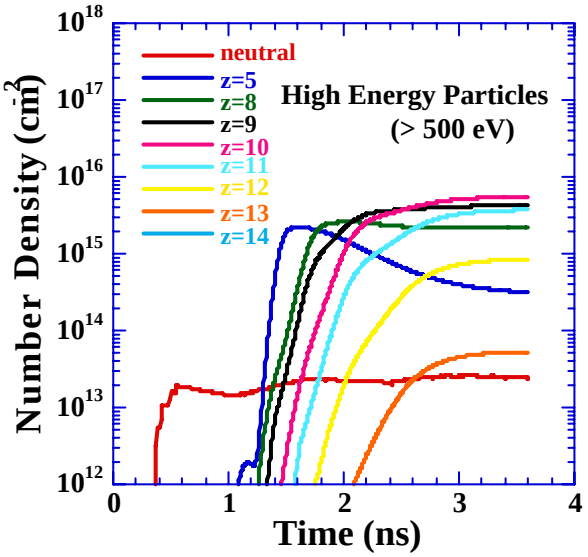

Fig. 3 (a) Time evolutions of number densities of high energy (more than 500eV) particles of each charges (includes neutral particles) of ablated materials.

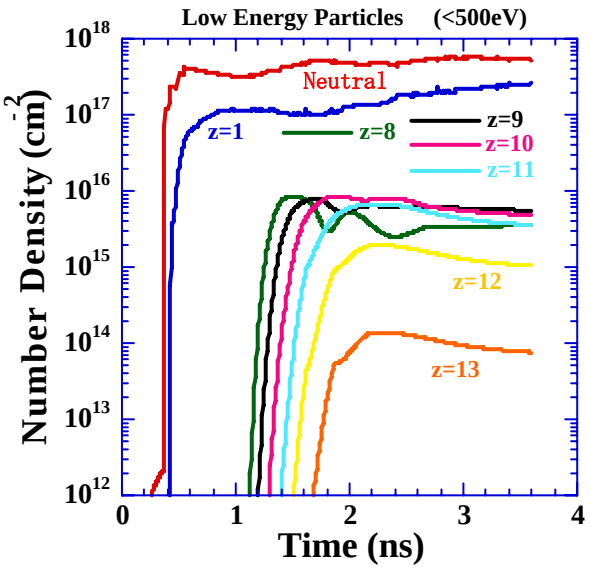

Fig. 3 (b) Time evolutions of number densities of low energy (less than 500eV) particles of each charges (includes neutral particles) of ablated materials.

Fig. 4 shows total (includes neutral particles) ion number density profile, electron temperature profile and Fig. 5 (a) shows number densities of high energy part using LAFRAC and for the case Saha-Boltzmann equilibrium at the time of laser end, and Fig. 5 (b) shows those of low

energy part using LAFRAC and for the case Saha-Boltzmann equilibrium at the time of laser end. Note that when number densities for the case Saha-Boltzmann equilibrium is estimated, the profiles at the time of laser end obtained by LAFRAC (Fig. 4) is used. As shown in Fig. 5 (a) and (b), simulation results have many highly charged particles compared with equilibrium results because of long recombination time scale compared with laser pulse duration.

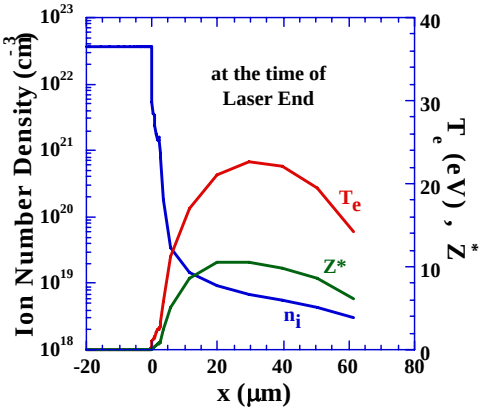

Fig. 4 Total (includes neutral particles) ion number density profile, electron temperature profile and ionization degree profile at the time of laser end.

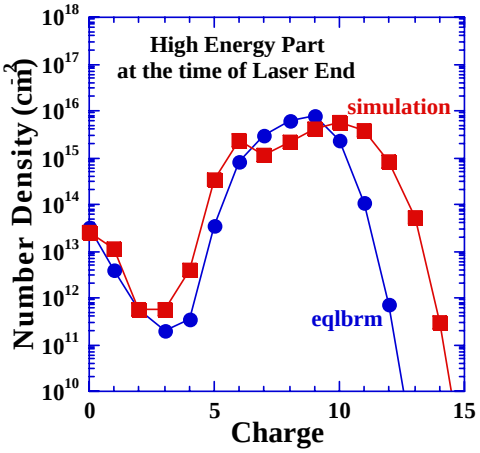

Fig. 5 (a) Number densities of high energy part using LAFRAC and for the case Saha-Boltzmann equilibrium at the time of laser end.

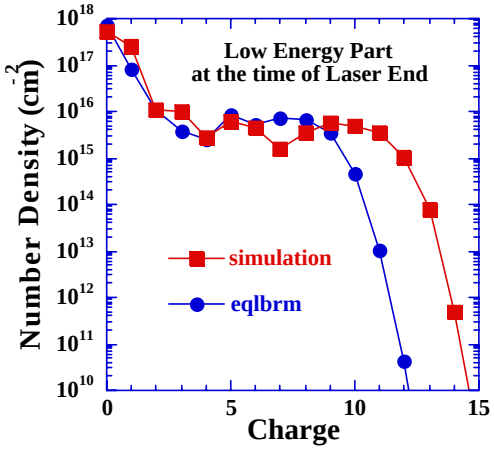

Fig. 5 (b) Number densities of low energy part using LAFRAC and for the case Saha-Boltzmann equilibrium at the time of laser end.

4. CONCLUDING REMARKS

An integrated Laser Ablation Fluid RAdiation simulation Code (LAFRAC)[1] has been developed to estimate behaviors of highly energetic ions and neutral particles from laser ablation produced plasmas, and to estimate ionization and recombination processes. LAFRAC includes effects of time dependent population kinetics[2], phase transition[3] from liquid to neutral gas to partially ionized plasma, detail laser absorption processes[4], hydrodynamics, and radiation transport.

A laser ablation simulation using LAFRAC is performed. In this simulation, laser peak intensity is 10^{11} W/cm^2, pulse duration is 1.2 ns, and material is tin.

Time evolutions of ablation depth are estimated. As shown in previous section, evaporation and peeling occur for this condition.

Time evolutions of number densities of each charges (includes neutral particles) of ablated materials. As shown in previous section, particles of which charges 8 to 11 are dominant for high energy part, and particles of which charges 0 to 1 are dominant for low energy part. Note that number density of neutral particles of low energy part is almost100 times of that of particles of which charge 10 of high energy part. Almost of all ablated materials are neutral particles.

Number densities of high energy part using LAFRAC and for the case Saha-Boltzmann equilibrium at the time of laser end, and those of low energy part using LAFRAC and for the case Saha-Boltzmann equilibrium at the time of laser end are shown in previous section. Simulation results have many highly charged particles compared with equilibrium results because of long recombination time scale compared with laser pulse duration.

In future work, I would like to calculate for long time (after laser irradiation finishes), and compare with experimental results, for example results in ref. 8.

REFERENCES

[1] H. Furukawa et. al., Proc. SPIE **5448** (2004) 872-884
[2] T. Kawamura, Doctor thesis (1999) in Japanese.
[3] S. I. Anisimov, and B. S. Luk'yanchuk, Physics-Uspekhi **45** (2002) 293-324
[4] M. V. Allmen, and A. Blatter, " Laser-Beam Interactions with Materials", Springer
[5] M. Ito, and T. Yabe, Phys. Rev. A **35** (1987) 233-241.
[6] Vivek Bakshi edit., ' EUV Sources for Lithography SPIE Publications (2006) ISBN 0-8194-5845-7
[7] Y. Tao et. al.; Appl. Phys. Lett. **86** (2005) 201501
[8] S. Fujioka, et. al.:, Appl. Phys. Lett. **87** (2005) 241503..

(Received: May 17, 2006, Accepted: November 15, 2006)